Jurnal Teknologi, 55 (Sains & Kej.) Keluaran Khas (1), Mei 2011: 17–30

GRADIENT-INDEX FIBRE BASED MINIATURE GAS CELL FOR INTRA-CAVITY FIBRE LASER SENSORS

MO LI[1*], ASRUL IZAM AZMI[1] & GANG-DING PENG[1]

Abstract. This paper presents a new and simple design of gas cell for the use of intra-cavity fibre laser sensors. This design utilizes gradient-index fibres for collimation to realize a miniature gas cell of very small diameter. By using the Gaussian field approximation and ray transformation, the gas cell is analyzed and optimized. It is found that gradient-index fibre based cells could achieve lower coupling loss of nearly 10 dB at a separation of 20 mm and allow for additional tolerance to certain misalignments, in comparison with those single-mode fibre based cells. A new-design cell is fabricated and its coupling loss is tested with a 1550 nm laser. Good agreement in the analysis and experimental results is obtained, indicating that the design could be feasible in practical gas sensing.

Keywords: Gradient-index fibre based cell; gradient-index fibre collimator (GIFC); coupling loss; misalignments; intra-cavity fibre gas sensor

1.0 INTRODUCTION

Intra-cavity absorption gas sensors have attracted a lot of research interests with enhanced sensitivity by inserting a gas cell into the laser cavity [1]. For these kinds of gas sensors, gas cell is one of the most critical components, the length and volume of which both affect the sensitivity, stability and other performances of the sensor. One of the key considerations of the gas cell is the collimation techniques, which help improve the utilization ratio of the light source, reduce the coupling loss and increase the coupling efficiency.

Conventional gas cells always utilize direct single-mode fibre (SMF) fibre-to-fibre coupling methods or gradient-index (GRIN) glass lenses as the collimators. Direct fibre-to-fibre gas cell has simple configuration, but suffers from high coupling loss. Gas cells employing GRIN rod lenses are advantageous to achieve low coupling loss while it always combined with bulky lenses and requires

[1] School of Electrical Engineering and Telecommunications, University of New South Wales, Sydney, 2052, Australia

[*] Corresponding author: limomaria@yahoo.cn

alignments which could compromise long term reliability and stability. Also, the GRIN rod lenses cannot be glued directly to the fibre, thus mechanical instability caused by thermal expansion of the optical fibre is unavoidable and not suitable for environments with narrow space or high temperature [2-3]. In order to overcome those problems, in our design, we utilize a pair of one-quarter pitch gradient-index fibre collimators (GIFC) to build a cell. This cell is very compact, and has the ability to have good stability and easy alignment.

In this paper, the design and the fabrication process of this GIFCs based cell is firstly introduced. To have better understanding of its characteristics, we analyze the coupling losses of it induced by misalignments between GIFCs based on Gaussian field approximation and ray propagation. Formulas and numerical simulation results are presented. Experiments are also conducted and the results agree well with the prediction which means the analysis is adequate for describing the coupling performances and could prove the practical feasibility of the design.

2.0 GAS CELL DESIGN AND FABRICATION OF THE GAS CELL

GIFC: Traditional gas cells for fibre sensors use direct fibre-to-fibre coupling methods or GRIN glass lenses as the collimators. For the reasons mentioned above, we propose the new designed gas cell using GIFC. GRIN fibre has a core whose gradient constant varies with the distance from the fibre axis, as to be described in next section; it has a lens-like effect to collimate the light that enables us to fabricate a GIFC with a proper length of GRIN multimode fibre fused with a SMF. A pair of GIFCs can make a miniature fibre-pigtailed gas cell that has the advantages of improved coupling efficiency (compared with direct SMF-to-SMF coupling), small size, low cost and stable fibre-GIFC interface.

We tested the effectiveness of GIFC for producing collimated beams by using the setup shown in Figure 1. Here we measured the far-field patterns of the beam out of the GIFC and the SMF.

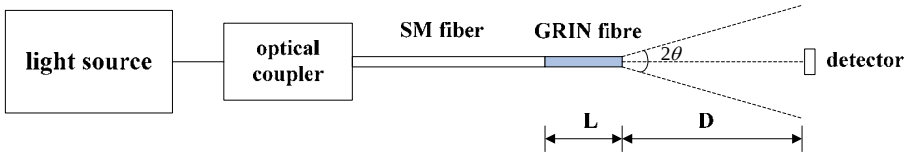

Figure 1 Setup of measuring the far-field pattern of GRIN fibre and SMF

The gradient constant of GIFC we use is g = 6.3626 mm^{-1} with a period length of about 0.99 mm. Because the 1/4 pitch length of our GRIN fibre is small which is

inconvenient for practical experiments, we choose longer GRIN fibre with odds times of quarter-pitch length. The final length we use is 14.68 mm. The distance D between the detector and the fibre end is 75 mm.

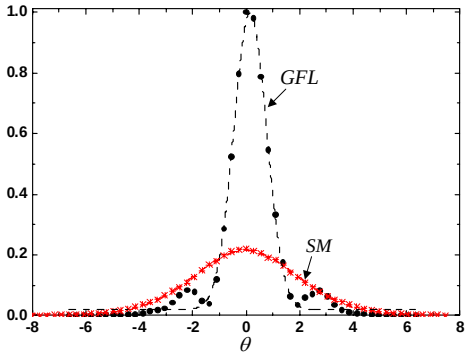

Figure 2 Experimental results of far-field distribution pattern of GRIN fibre and SMF

The result of far-field measurement is illustrated in Figure 2. The lateral axis represents the divergence angle of the basic mode field of the fibre; the longitudinal axis is the normalized amplitude of the beam intensity detected. The discrete points are experimental results and the dashed lines are curves fitted by Gaussian profiles. The fluctuations of the GRIN fibre experimental results may due to the influence of other modes of GRIN fibre.

From Figure 2 it is clear that, the divergence angle of the basic mode of GIFC is much smaller than that of SMF. The beam intensity detected at the same distance is much greater. This means, by using GIFC into the cell, the beam could transmit with a smaller divergence angle in longer distance. This characteristic allows the gas cell have longer absorption length which will induce better detection sensitivity without sacrificing the light power.

Fibre ring laser and gas cell: Our gas sensing system is a typical intra-cavity gas sensor, including: a 980 nm diode pump, a 980/1550 WDM coupler, an EDF gain media, an isolator, a tunable filter, a coupler, a tunable attenuator and a gas cell (Figure 3 (a)).

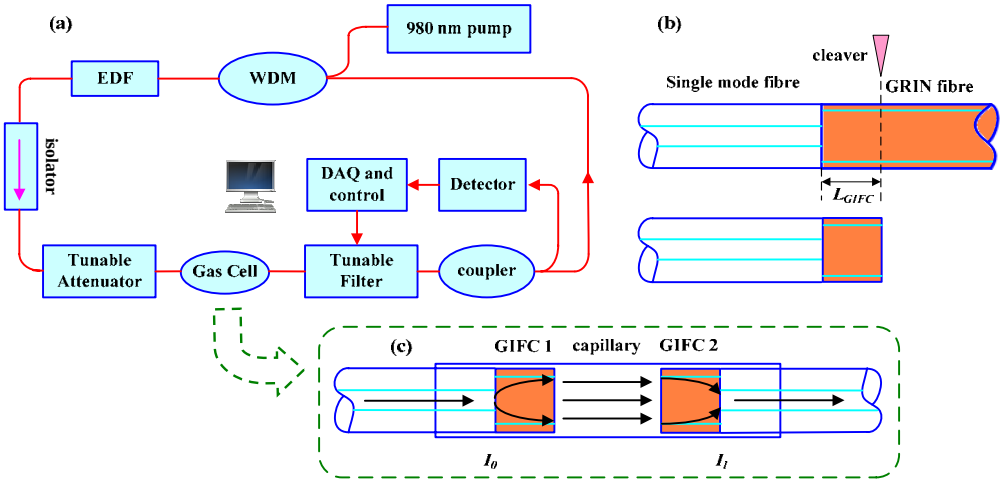

Figure 3 (a) The configuration of the gas sensor; (b) the fabrication of GIFC; (c) the structure of GRIN fibre based cell and the propagation of the beam in the cell

The gas cell is a transmission type cell. By inserting GIFCs into a capillary which has similar diameter, the gas cell is made very thin and miniature. The stable (fused) fibre interface also makes it feasible for extreme environment with narrow space and high temperature.

The procedure of the GIFC fabrication is shown in Figure 3(b). Using a commercial splicer, the GRIN fibre is spliced with SMF and then one-quarter pitch cleaved ($L_{GIFC} = \frac{1}{4} pitch$). The structure is shown in Figure 3(c). For this kind of gas cell, the output can be expressed as [4-5]:

$$I_1 = I_0 \eta \exp\left[-\alpha(\nu) L C\right] \tag{1}$$

where I_0 and I_1 is the intensity of the light before and after passing through the gas cell, η is the loss of the gas cell, L is the length of the gas cell and $\alpha(\nu)$ is the absorption coefficient.

Figure 3(c) also illustrates the propagation of the beam transmitting through the gas cell. When the beam transmits from SMF, it is collimated by GIFC 1. After passing through the air gap between the two collimators, the beam is focused by GIFC 2. The loss analysis is given in the following part.

3.0 GAS CELL ANALYSIS

3.1 Ray analysis of GIFC

A square-law GIFC has a refractive index dependant on its radical distance. The refractive index get its largest value along the longitudinal axis and decreases with radial distance which is given by [6]:

$$n^2(r) = n_0^2(1 - g^2 r^2) \tag{2}$$

where n_0 is the refractive index along the axis, g is the gradient parameter and r is the radial distance from the axis [7]. Figure 4 shows the refractive profile of GIFC and the beam propagating through it [8]. The ray path in GIFC is a sinusoidal profile with the period given by:

$$L = \frac{2\pi}{g} \tag{3}$$

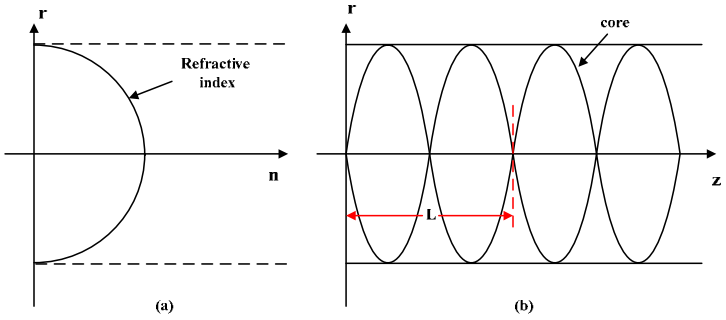

Figure 4 (a) Refractive index profile of GIFC; (b) ray path in GIFC

The position and the slope of the ray propagating through GIFC can be described by the ray-transfer matrix (ABCD matrix) [7].

$$\begin{pmatrix} r_{out} \\ r'_{out} \end{pmatrix} = \begin{pmatrix} \cos(gz) & \sin(gz)/n_0 g \\ -n_0 g \sin(gz) & \cos(gz) \end{pmatrix} \begin{pmatrix} r_{in} \\ r'_{in} \end{pmatrix} \tag{4}$$

where z is the length of GIFC, r_{in} and r'_{in} are the position and slope of the input ray just inside GIFC, r_{out} and r'_{out} are the position and slope of the exit ray.

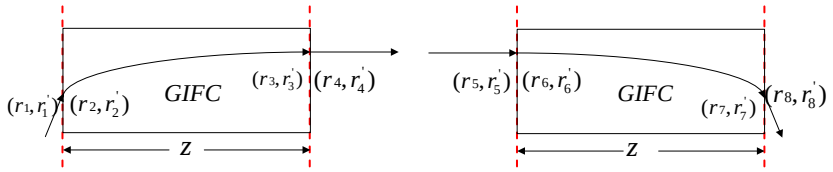

Figure 5 Path of a light beam through the transmitting and receiving GIFCs.

As is shown in Figure 5, $z = \frac{1}{4} pitch = \frac{\pi}{2g}$. For the transmitting GIFC, we can obtain:

$$r_4 = \frac{1}{n_0 g} r_1' \qquad (5)$$
$$r_4' = -n_0 g r_1$$

The junction of the SMF and GIFC is approximated as a point light source, so $r_1 = r_2 = 0$. Using Eq. 5, we could obtain that $r_4' = 0$. It reveals that the rays passing through 1/4 pitch GIFC from the axis are collimated. For the receiving GIFC, $r_5' = 0$ and $r_7 = r_8 = 0$, which indicates that the collimated beam is converged to the axis. Hence for a GIFC, with length P given by Eq.6, the light beam will be collimated from a point light source and can be used as collimator.

$$P = (2k+1)L/4, \quad k = 0,1,2,\cdots \qquad (6)$$

3.2 Coupling loss of GIFCs

There are three types of misalignments of the gas cell between GIFCs [9] as are shown in Figure 6: (1) separation between GIFC ends; (2) lateral offset between the longitudinal axes of GIFCs; (3) angular tilt between the longitudinal axes of GIFCs.

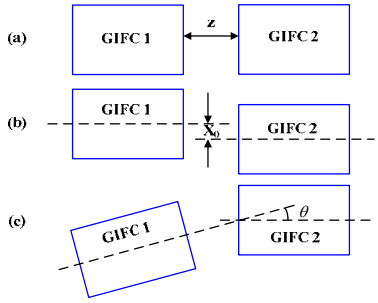

Figure 6 Three types of misalignments: (a) separation; (b) lateral offset; (c) angular tilt

The coupling loss analysis utilizes the ray matrix transformation of the complex beam parameters. The radius of curvature of the Gaussian beam is $R(z)$, the spot size is $\omega(z)$ and the complex beam parameter is $q(z)$, they satisfy the relation as follows [2, 10]:

$$\frac{1}{q(z)} = \frac{1}{R(z)} - i\frac{\lambda}{\pi\omega^2(z)} \tag{7}$$

where λ is the wavelength of the light.
The transformation of $q(z)$ through a GIFC satisfies the ABCD law:

$$q_2 = \frac{Aq_1 + B}{Cq_1 + D} \tag{8}$$

where q_1 and q_2 are the complex beam parameters of the input and output planes. In combination with 1/4 pitch GIFC, we could obtain:

$$\begin{pmatrix} A & B \\ C & D \end{pmatrix} = \begin{pmatrix} 0 & 1/n_0 g \\ -n_0 g & 0 \end{pmatrix} \tag{9}$$

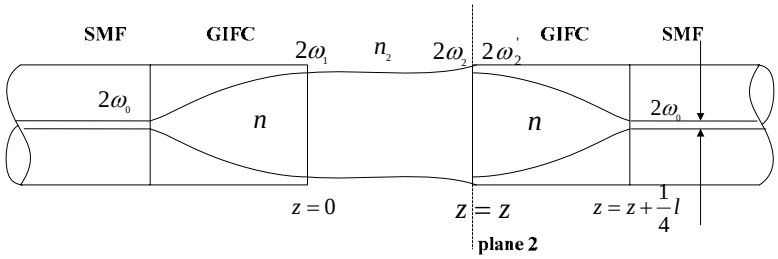

Figure 7 Propagation of a Gaussian beam through GIFC.

As Figure 7 shows, considering the Gaussian field diameter emitted from the SMF as ω_0, $R_0 = \infty$, the radius of the beam diverging from GIFC becomes:

$$\omega_1 = \frac{\lambda}{\pi n_0 g \omega_0} \tag{10}$$

where n_0 is the refractive index on the axis.
If we assume ω_1 is the waist radius, n is the refractive index of the air gap, the beam radius ω_2 at z is [11]:

$$\omega_2 = \omega_1 \left\{ 1 + \left[\frac{z\lambda}{\pi n \omega_1^2} \right]^2 \right\}^{1/2} \tag{11}$$

$$R_2(z) = z \left\{ 1 + \left[\frac{\pi n \omega_1^2}{\lambda z} \right]^2 \right\} \tag{12}$$

If we assume the beams couple at plane 2 and $\omega_2^{'}$ is the waist radius, we can get:

$$\omega_2^{'} = \frac{\lambda}{\pi n_0 g \omega_0} \tag{13}$$

$$R_2^{'} = \infty \tag{14}$$

By assuming the emerging field as Gaussian field, the field distribution can be written in the form[12]:

$$\psi(r,z) = A(z) \exp\left[-\left(\frac{r-\Delta}{\omega(z)} \right)^2 \right] \times \exp\left[-i \frac{k(r-\Delta)^2}{2R(z)} \right] \exp\left[-i(kz - \omega^{'} t) \right] \tag{15}$$

where ω is the beam radius, $R(z)$ is the radius of curvature, $A(z)$ is the amplitude, Δ is the transverse offset, $k = 2\pi / \lambda$, $\omega^{'} = \tan^{-1}\left(\frac{\lambda z}{\pi n \omega^2} \right)$.

Coupling versus separation: If there is no offset misalignment or angular tilt between GIFCs, the mode field of ω_2 and $\omega_2^{'}$ in Figure 7 can be expressed as:

$$\psi_2(r,z) = A(z) \exp\left[-\left(\frac{r}{\omega_2} \right)^2 \right] \times \exp\left[-i \frac{kr^2}{2R_2(z)} \right] \exp\left[-i(kz) \right] \tag{16}$$

$$\psi_2^{'}(r,z) = B(z) \exp\left[-\left(\frac{r}{\omega_2^{'}} \right)^2 \right] \tag{17}$$

The on-axis coupling efficiency is determined by the overlap of the two Gaussian beams at z [9]:

$$\eta = \frac{\left| \iint \psi_1(r,z) \psi_2^*(r,z) dxdy \right|^2}{\iint \psi_1(r,z) \psi_1^*(r,z) dxdy \iint \psi_2(r,z) \psi_2^*(r,z) dxdy} \tag{18}$$

Combined with Eq.16 and Eq.17, coupling efficiency can be expressed as follows:

$$\eta = \frac{4}{\left(\frac{\omega_2}{\omega_2'} + \frac{\omega_2'}{\omega_2}\right)^2 + \left(\frac{k\omega_2\omega_2'}{2}\right)^2 \left(\frac{1}{R_2} - \frac{1}{R_2'}\right)} \tag{19}$$

Coupling loss in units of decibels could be expressed as:

$$L = -10\log\eta \tag{20}$$

As a comparison, if there are no collimators in the gas cell, that is, the gas cell is based on direct SMF-SMF coupled techniques; the spot size and the curvature radius of the illumination beam along the z-axis are given by:

$$\omega_1 = \omega_0 \left\{1 + \left[\frac{z\lambda}{\pi n \omega_0^2}\right]^2\right\}^{1/2} \tag{21}$$

$$R_1 = z\left\{1 + \left[\frac{\pi n \omega_0^2}{z\lambda}\right]^2\right\} \tag{22}$$

where ω_0 is the modal field radius of SMF and also is the beam waist radius.

Assuming that the waist is on the output plane, the radius of curvature is infinite, the coupling loss between two SMFs (in Figure 8) can be written as[13]:

$$L = -10\log\eta = -10\log\left(\frac{4}{\left(\frac{\omega_1}{\omega_0} + \frac{\omega_0}{\omega_1}\right)^2 + \frac{k^2}{4R_1^2}\omega_0^2\omega_1^2}\right) \tag{23}$$

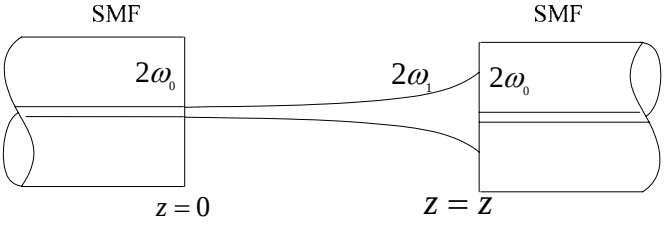

Figure 8 The beam propagation between SMFs

Coupling versus lateral offset misalignment and angular tilt: The analysis of GIFCs coupling loss due to lateral offset (X_0) (no separation

misalignment and angular tilt) and angular tilt (θ) (no separation and offset misalignment) are similar and the expressions can be expressed as [7, 14]:

$$L_{offset,z=0,\theta=0} = 4.343\left(\frac{\pi n_0 g \omega_0 X_0}{\lambda}\right)^2 \tag{24}$$

$$L_{tilt,z=0,X_0=0} = 4.343\left(\frac{\tan\theta}{n_0 g \omega_0^2}\right)^2 \tag{25}$$

4.0 RESULTS AND DISCUSSIONS

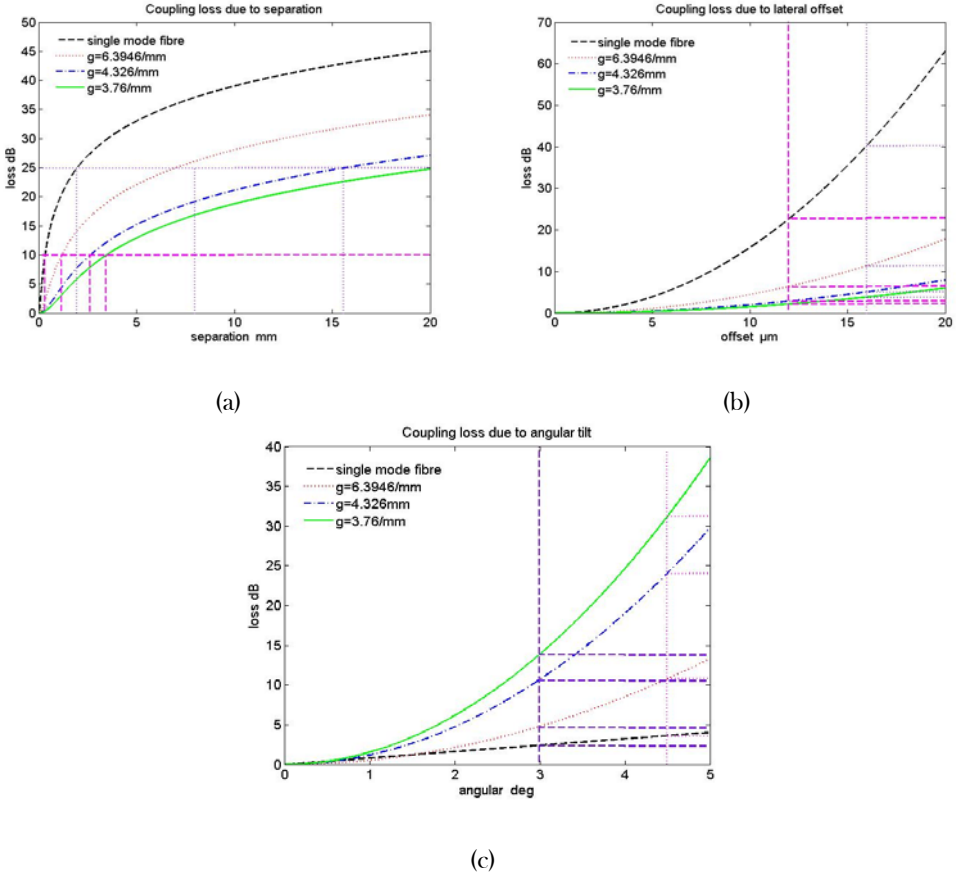

Figure 9 Prediction of coupling losses due to three types of misalignments: (a) separation z (mm); (b) lateral offset X_0 (μm); (c) angular tilt θ(degree)

Simulations of coupling losses versus the separation, offset and the angular tilt between the GIFCs, for varying gradient constant (g) are shown in Figure 9. The coupling losses between SMFs (without GIFCs) are also included in this figure for comparison.

For the coupling loss induced by separation between the fibre ends, from Figure 9 (a), it is clear that if we hope the coupling loss of the gas cell to be less than 10 dB, the maximum separation of the fibre ends should be less than 0.2 mm, 1 mm, 2.5 mm and 3.5 mm for SMF, GIFC with g=6.3946 mm^{-1}, g=4.326 $mm^{-1}$and g=3.76 mm^{-1}, respectively. If we hope the coupling loss to be less than 25dB, the maximum separation between the fibre ends should be less than 2.3 mm, 7.8 mm, 15.5 mm and 20 mm for SMF, GIFC with g=6.3946 mm^{-1}, g=4.326 mm^{-1} and g=3.76 mm^{-1}, respectively. The lower the gradient constant g is, the lower the coupling loss will be and the longer separation length could be used for the gas cell, which means the increase of the gas detection sensitivity.

For the coupling loss induced by lateral offset (in Figure (b)), it is clear that the coupling loss increases with greater lateral offset; GIFC with lower gradient constant has lower coupling loss due to this misalignment. When the offset is 12 μm, the coupling loss is 2 dB, 3 dB, 6.5 dB and 22 dB for GIFC with g=3.76 mm^{-1}, g=4.326 mm^{-1}, g=6.3946 $mm^{-1}$and SMF respectively. When the offset is 16 μm, the coupling is 3.5 dB, 5 dB, 11.5 dB and 40 dB for GIFC with g=3.76 mm^{-1}, g=4.326 mm^{-1}, g=6.3946 $mm^{-1}$and SMF respectively. We can see using low gradient constant GIFC can effectively reduce the coupling loss than using SMF.

For the coupling loss induced by angular tilt, greater tilt will induce higher coupling. However, the variation is quite different with the former two. We find that using SMF could be influenced least by angular tilt. For GIFC, the higher the gradient constant g is, the lower coupling loss it will introduce. When the angular is 3 deg, the coupling loss of SMFs and GIFCs with g=6.3946 mm^{-1}, g=4.326 mm^{-1}, g=3.76 $mm^{-1}$is 2.5 dB, 5 dB, 10 dB and 14 dB respectively. When the angular is 4.5 deg, the respective coupling is 4 dB, 10.5 dB, 24.5 dB and 31.5 dB. The coupling loss of SMFs is much smaller than that of GIFCs at the same angular.
The simulation results also illustrate that, for a particular gradient constant, the coupling loss of GIFCs is least dependent on separation and most dependent on angular tilt. The low coupling loss sensitivity of GIFCs to separation allows for long cell length for increased gas sensitivity. It is also clear that gas cells based on GIFCs could have higher tolerance for separation and lateral offset than those based on SMFs. However, they have lower tolerance for angular tilt.

The coupling loss experiments with a 1550 nm laser source are conducted to examine the agreement of the analysis and the real situation. GRIN fibres with n_0=1.4875, g =6.3946 mm^{-1} and a core diameter of 62.5 μm were spliced and cleaved into a length of one quarter pitch. The SMF has a 9 μm core and 10.5 μm mode-field diameter. The fibres are fixed on the three dimensional micro-

positioner so that the separation between two fibre ends could be adjusted. The coupling losses are measured as a function of axial separation between the fibre ends.

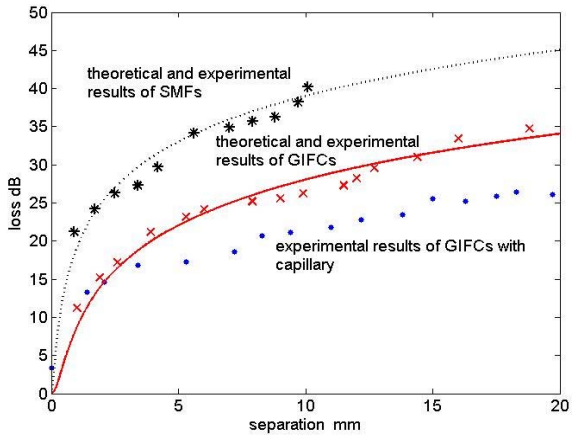

Figure 10 Comparison of experimental and theoretical results due to the separation between fibres in the cases: (a) between SMFs; (b) between GIFCs with capillary cell; (c) between GIFCs without capillary cell

Thus the coupling loss between a pair of SMFs, a pair of GIFCs with the capillary and a pair of GIFCs without the capillary were measured. From Figure 10 we can see, the coupling losses measured of GIFCs is lower than that of SMFs. The difference is nearly 10 dB at a separation of 20 mm. The experimental results conducted without the capillary agree well with the analysis. It means that our GRIN fibre based cell have much lower coupling loss in certain extent. However, there is a mismatch between the theory and experimental results conducted with the capillary cell. In that case, the experimental results are much lower than the prediction and the results of the experiments conducted without the capillary. This phenomenon is due to the influences of the stray light reflected by the inner wall of the capillary. However, in our simulation, we only simulate the ideal case without considering the reflection effects. The reflection decreases the coupling loss but induce the interference at the same time. In reality, the effects could be reduced by applying anti-reflection coatings to the inner wall of the capillary.

5.0 CONCLUSIONS

In this paper, a design of thin and stable GRIN fibre based gas cell is introduced. The advantages of this design include: low cost, compactness, easily alignment with

stable interfaces, which make it suitable for fibre sensing applications with high temperature or narrow space. Analyses and formulas for predicting the coupling losses of the gas cell are presented. Numerical simulations are performed with different gradient constants. Experiments are carried out with a 1550 nm laser source and GRIN fibre with g =6.3946 mm^{-1}. The experimental results agree well with the prediction with a separation distance in the range of 20 mm without the capillary. Experiments in the capillary are also conducted and analysis is given out to study the deviation between the prediction and the test results. The whole work proved that the GRIN fibre used as collimator in our gas cell could effectively reduce the coupling loss than that without it with better alignment tolerance of separation and offset which make the sensing system have the potential to have good detection sensitivity. The analysis is also able to describe the coupling characteristics of the gas cell and proves it has reasonable prospects in fibre sensing.

ACKNOWLEDGMENTS

Authors acknowledge funding of China Scholarship Council (No. 2008612037)

REFERENCES

[1] V.M.Baev, *et al.,* 1999. Laser Intra Cavity Absorption Spectroscopy. *Appl. Phys. B*. 69(3): 171-202.

[2] C. Gomez-Reino, *et al.,* 2008. Design of GRIN Optical Components for Coupling and Interconnects. *Laser & Photonics Reviews*. 2: 203-215.

[3] T. Sakamoto, 1992. Coupling Characteristic Analysis of Single-Mode and Multimode Optical-Fiber Connectors Using Gradient-Index-Rod Lenses. *Applied Optics*. 31: 5184-5190.

[4] J. M. Sa, *et al.,* 2007. Gas Cell Based on Cascaded GRIN Lens for Optical Fiber Gas Sensor. *3rd International Symposium on Advanced Optical Manufacturing and Testing Technologies: Optical Test and Measurement Technology and Equipment*. Parts 1-3. 6723: I7234-I7234

[5] J. Zhang, 2006. Design and Experiments of Optical Fibre Methane Gas Sensor. *Disseration for Doctoral Degree in Engineering*. Yanshan University (in Chinese).

[6] YU-Long Tang, *et al.,* 2008. Beam Collimation of High Power Laser Diode Array With Graded-Index Fibre Lens Array. *Opt.Eng*. 47(5).

[7] R. W. Gilsdorf and J. C. Palais, 1994. Single-Mode Fiber Coupling Efficiency with Graded-Index Rod Lenses. *Applied Optics*. 33: 3440-3445.

[8] S. H. Wang, *et al.,* 2002. Study of Collimating Laser Diode Beam by a Graded-index Optical Fibre (vol 112, pg 533, 2001). *Optik*. 113: 103-103.

[9] S. F. Yuan and N. A. Riza, 1999. General Formula for Coupling-loss Characterization of Single-mode Fiber Collimators by Use of Gradient-index Rod Lenses. *Applied Optics*. 38: 6292-6292.

[10] W. L. Emkey and C. A. Jack, 1987. Analysis and Evaluation of Graded-Index Fiber-Lenses. *Journal of Lightwave Technology*. 5: 1156-1164.

[11] J. C. Palais, 1980. Fiber Coupling Using Graded-Index Rod Lenses. *Applied Optics*. 19: 2011-2018.

[12] D. G. Hall, *et al.,* 1979. Simple Gaussian-Beam Model for Gaalas Double-Heterostructure Laser-Diode-to-Diffused-Waveguide Coupling Calculations. *Optics Letters*. 4: 292-294.

[13] Mo Li, *et al.,* 2009. Thin Gas Cell with GRIN Fiber Lens for Intra-cavity Fiber Laser Gas Sensors. *International Symposium on Photoelectronic Detection and Imaging 2009: Laser Sensing and Imaging, Proc of SPOE*. Vol. 7382, Beijing.

[14] Mo Li, *et al.,* 2009. Analysis and Experiment of Gradient-Index Fibre Collimators for Fibre Sensing. *Australiasian Conference on Optics, Lasers and Spectroscopy and Australian conference on Optical Fibre Technology in association with the International Workshop on Dissipative Solitons (ACOFT)*. Adelaide.